Molecular Cell
Article

Mechanism of Homology Recognition in DNA Recombination from Dual-Molecule Experiments

Iwijn De Vlaminck,[1] Marijn T.J. van Loenhout,[1] Ludovit Zweifel,[1] Johan den Blanken,[1] Koen Hooning,[1] Susanne Hage,[1] Jacob Kerssemakers,[1] and Cees Dekker[1,*]
[1]Kavli Institute of Nanoscience, Delft University of Technology, Lorentzweg 1, 2628 CJ Delft, The Netherlands
*Correspondence: c.dekker@tudelft.nl
DOI 10.1016/j.molcel.2012.03.029

SUMMARY

In *E. coli* homologous recombination, a filament of RecA protein formed on DNA searches and pairs a homologous sequence within a second DNA molecule with remarkable speed and fidelity. Here, we directly probe the strength of the two-molecule interactions involved in homology search and recognition using dual-molecule manipulation, combining magnetic and optical tweezers. We find that the filament's secondary DNA-binding site interacts with a single strand of the incoming double-stranded DNA during homology sampling. Recognition requires opening of the helix and is strongly promoted by unwinding torsional stress. Recognition is achieved upon binding of both strands of the incoming dsDNA to each of two ssDNA-binding sites in the filament. The data indicate a physical picture for homology recognition in which the fidelity of the search process is governed by the distance between the DNA-binding sites.

INTRODUCTION

RecA from *E. coli* is the prototype of a family of recombinases essential in double-stranded (ds)DNA break repair and recombination (Kowalczykowski et al., 1994). RecA forms a nucleoprotein filament on a single-stranded (ss)DNA that searches and pairs a homologous sequence within another, double-stranded DNA molecule (Radding, 1991). The search for homology conducted by the RecA filament poses a formidable challenge from a kinetic and thermodynamic point of view (Barzel and Kupiec, 2008). The RecA filament is able to detect a short homologous sequence of DNA embedded in genomic-length dsDNA (Hsieh et al., 1992). The search process is completed within the timescale set by the cell's life cycle, implying an impressive $>10^3$ s^{-1} base-sampling frequency (Camerini-Otero and Hsieh, 1993). Homology search is little affected by a large background of heterologous DNA (Honigberg et al., 1986), suggesting that the filament is somehow able to cope with the abundantly present short sequences in the genome that display heterology or partial homology.

With these characteristics, the RecA homology search is an example of a general class of target-localization processes commonly encountered in molecular biology in which a recognizing molecule finds a specific target among many look-alikes in a noisy background (Savir and Tlusty, 2007, 2010). Recently, it was proposed that conformational proofreading is used as a general strategy in target localization (Savir and Tlusty, 2007). Here, a conformational mismatch between the target-bound and unbound states improves the selectivity of the process by necessitating the recognizing molecule to access an energetically unfavorable intermediate state during proofreading. For the RecA homology search, this raises questions about how the structure of the minimally stable target-bound state is defined and which intermediate states are transiently accessible during proofreading.

Proofreading or homology sampling occurs via Watson-Crick-type base pairing of the bases of the incoming dsDNA with the bases of the ssDNA in the primary binding site at the center of the filament (Chen et al., 2008; Folta-Stogniew et al., 2004). The filament has a secondary DNA-binding site (SBS) that mediates the homology sampling reaction (see inset in Figure 1A). Two different mechanistic models for the function of the SBS during the homology sampling reaction have been proposed in which the SBS binds the incoming dsDNA in structurally distinct intermediate states. The first model assumes that the SBS destabilizes the incoming dsDNA upon binding of dsDNA into an extended and underwound conformation, thereby facilitating base sampling (Danilowicz et al., 2011; Dorfman et al., 2004; Mani et al., 2010; Rould et al., 1992; Sagi et al., 2006; Savir and Tlusty, 2010). A second model assumes that the SBS binds to one of the strands of the dsDNA, leaving the second strand available for base sampling (Chen et al., 2008; Folta-Stogniew et al., 2004; Voloshin and Camerini-Otero, 2004). Here, it is not clear whether the filament has an active role in dsDNA helix opening or whether homology recognition relies on intrinsic DNA-breathing dynamics (Folta-Stogniew et al., 2004; Voloshin and Camerini-Otero, 2004).

Homology sampling and recognition constitute difficult-to-isolate intermediate steps in a complex pathway that includes RecA filament formation, initial homologous alignment, strand exchange and strand displacement (Kowalczykowski et al., 1994; Radding, 1991). Complexes formed at sites of heterology and early recognition products are inherently short-lived and therefore difficult to investigate (Müller et al., 1990). Consequently, the structure of the minimally stable recognition product and the role of the SBS in homology sampling have proven challenging to resolve.

Here, we isolate and study binding interactions relevant in homology recognition using a dual-molecule manipulation

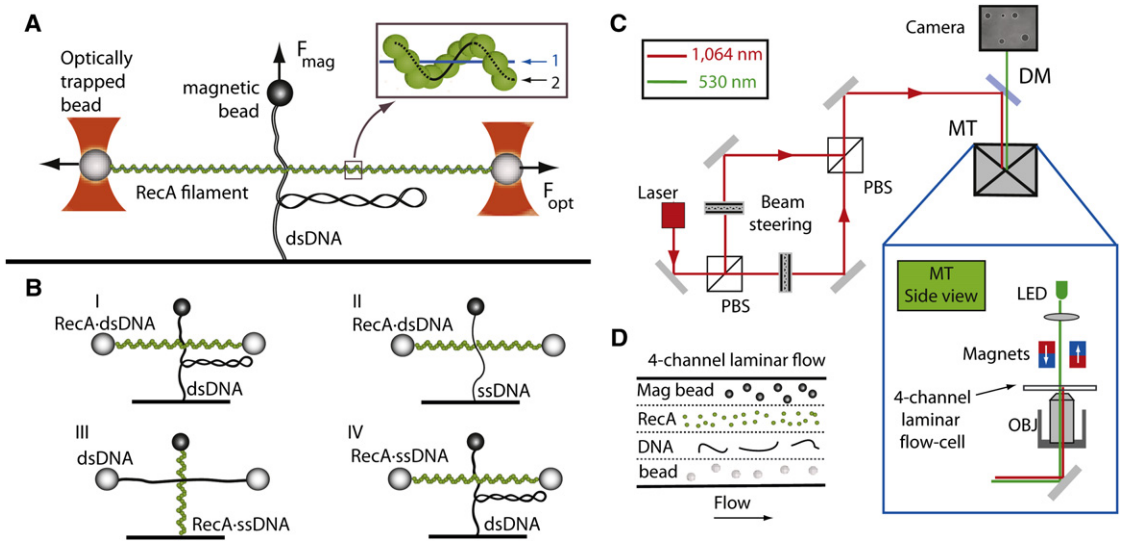

Figure 1. Experimental Approach

(A) Side view of dual-molecule assay where a RecA filament that is held in the optical tweezers interacts with a coiled dsDNA that is tethered in a magnetic-tweezers configuration. Inset: schematic of the RecA filament represented with two DNA-binding sites, a primary site (1) and secondary DNA-binding site (2).

(B) The four different experimental configurations I–IV used in this work.

(C) Schematic outline of the setup indicating the main components (for a more detailed description see Figure S1). Two independently steerable optical traps are generated using a 1064 nm laser system. The beams are split and recombined using a polarizing beam splitter (PBS) and focused using a high numerical aperture objective (OBJ) in the volume of a four-channel laminar-flow cell. Positioning and rotation of an external magnet pair allows stretching and coiling of a molecule tethered in the magnetic tweezers configuration.

(D) Top view of the four-channel laminar-flow system used for the assembly of the molecular constructs. See also Figure S1.

technique (Figure 1). A combination of magnetic-tweezers and optical-tweezers-based single-molecule manipulation allows bringing two distinct molecules into local contact to investigate the strength and frequency of occurrence of binding interactions. We directly probe and compare interactions of RecA filaments formed on ssDNA or dsDNA with ssDNA and (non) supercoiled dsDNA, using the four different experimental configurations depicted in Figure 1B (panels I–IV). We present measurements of the probability and strength of intermolecular binding as well as measurements of friction arising between filaments and DNA during sliding of one molecule across the other.

We find that the affinity of the SBS for dsDNA is too weak to account for local stretching or unwinding of dsDNA during homology sampling. We confirm that the SBS has a strong preference for ssDNA (Mazin and Kowalczykowski, 1998), but we find that its affinity for ssDNA is too weak to stably trap ssDNA bubbles in dsDNA. We furthermore find homologous pairing is strongly promoted by negative supercoiling of the incoming dsDNA. All in all, the data indicate a model for recognition in which the SBS of the filament binds to a single strand of the incoming dsDNA during homology recognition. When both strands of the incoming dsDNA bind to each of the two independent ssDNA-binding sites in the filament, the SBS and the sequence-specific ssDNA in the core of the filament, a stable joint molecule can be formed and homology recognition can be achieved. We propose that the fidelity of the recognition process is governed by the distance between both DNA-binding sites.

RESULTS

Dual-Molecule Manipulation Assay

The dual-molecule molecule technique introduced here is a combination of dual-bead optical tweezers and magnetic tweezers. Figure 1C shows a schematic of the setup and its main components (see Supplemental Information for a more detailed description). Two independently steerable optical traps are generated in the sample. A DNA molecule or RecA filament is end-attached between two surface-functionalized polystyrene beads held in the optical traps. A stretching force can be applied to this molecule through independent movement of the traps. Simultaneous movement of the traps allows 3D-manipulation of this molecule in the proximity of a second molecule that is tethered in between the bottom of a flow cell and a paramagnetic bead in a magnetic tweezers configuration. Positioning and rotation of an external magnet pair allows stretching and coiling of this second molecule. The magnetic tweezers thus permit studying the effects of twist and torque on the intermolecular binding. The position of five beads, two optically trapped beads, the paramagnetic bead and two fiducial markers, are measured in real time during the experiments using video-microscopy (50–100 Hz, 0.5 nm accuracy per frame). The distances between the molecules are accordingly deduced. Intermolecular binding forces are determined on the basis of lateral deflections of the superparamagnetic bead (see Experimental Procedures). The superparamagnetic bead of the magnetic tweezers serves as a sensitive force probe, with a force-resolution that is only limited by the thermal force noise acting on the bead ($\sim$10fN/$\sqrt{\text{Hz}}$; see

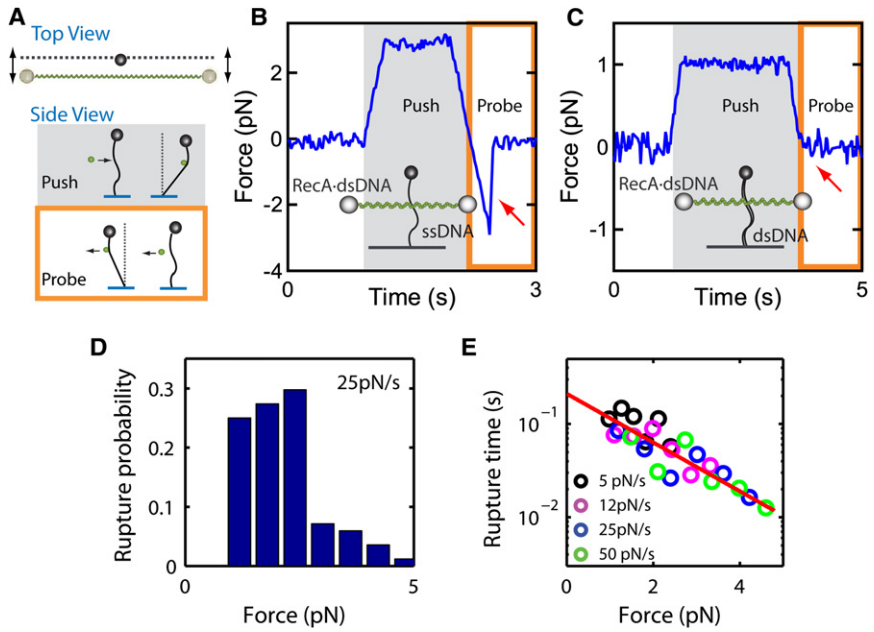

Figure 2. The Secondary Binding Site Binds ssDNA but Does Not Bind dsDNA

(A) Schematic shows a top view and a side view (along the filament) of the push and probe phases of a push-probe experiment. Forces were obtained from the deflection of the magnetic bead (see Supplemental Information).

(B) Push-probe experiments reveal binding of ssDNA to the secondary binding site of a RecA•dsDNA filament. A force of 2.9 pN is required to disrupt the intermolecular bond (red arrow). F_{mag} = 15 pN.

(C) Absence of binding of dsDNA (red arrow). F_{mag} = 2 pN.

(D) Rupture-force histogram from multiple push-probe measurements (n = 84) as in (B) (force ramp rate, dF/dt = 25 pN/s).

(E) Force-dependence of the bond lifetime of ssDNA bound to the SBS. The bond lifetime was obtained by converting data from rupture-force histograms measured at different ramp speeds using Equation 1. The red line is a fit of Bell's formula to the data, $\tau(F) = \tau_0 \exp(-Fx_b/kT)$; see text. See also Figure S2.

Supplemental Information). The force probe furthermore has ideal force-clamp characteristics (Strick et al., 2003). A four-channel laminar-flow cell (Noom et al., 2007; Wuite et al., 2000) was used for the independent, stepwise assembly of DNA molecules and RecA filaments tethered in the magnetic tweezers and optical tweezers, prior to interaction experiments. The flow system allows interaction experiments to take place under buffer conditions that can be chosen independently from the DNA and filament assembly buffers (see Supplemental Information). RecA assembly reactions were followed to completion and the mechanical properties of the various single-molecule constructs were characterized prior to interaction experiments (see Figures S1D– S1G).

Strength of Binding of Secondary Binding Site to ssDNA and dsDNA

We first examine the interactions of dsDNA or ssDNA molecules tethered in the magnetic tweezers with a RecA•dsDNA filament held in the optical tweezers (configuration I and II in Figure 1B). Since the bases of the double stranded DNA in the primary site within the RecA•dsDNA filament are inaccessible, interactions of incoming DNA with the filament are restricted to the SBS. The probability and strength of binding of dsDNA and ssDNA to the SBS are first investigated using a push-probe experimental approach where a contact between both molecules is first established by pushing the filament against the DNA and then disrupted by withdrawing to probe the strength of the intermolecular bond (see Figure 2A, and Movie S1).

We observe a strong binding of ssDNA to the SBS. The data in Figure 2B, for example, show a force of 2.9 pN required to disrupt the intermolecular bond. The strength of binding of ssDNA to the SBS of a RecA•dsDNA filament was quantified through an analysis of the statistical distribution of bond-rupture forces (Dudko et al., 2008; Evans, 2001). The rupture-force distribution is a function of the force ramp-rate, dF/dt (Figure S2). Figure 2D shows a rupture-force probability histogram, $p_F(F)$, acquired from multiple (n = 84) push-probe measurements as in Figure 2B, at a fixed force-ramp speed, dF/dt = 25 pN/s. $p_F(F)$ can be transformed into the force dependence of the bond lifetime $\tau(F)$ using (Dudko et al., 2008): $\tau(F) = \int_F^\infty (p(f)/((dF/dt)p(F)))df$. The data for $\tau(F)$ acquired at different dF/dt (5 to 50 pN/s) collapse onto a single master curve (Figure 2E) indicating that the rupture-force kinetics measurable at constant force behave as a single exponential (Dudko et al., 2008). Figure 2E shows a fit to the data of Bell's formula, $\tau(F) = \tau_0 \exp(-Fx_b/k_bT)$, where τ_0 is the zero-force bond lifetime, x_b is a distance to the transition state, k_b is the Boltzmann constant and T is the temperature (τ_0 = 0.2 s, x_b = 2.5 nm). To directly compare the free energy of binding of ssDNA to the SBS to the free energy of formation of a B-form DNA duplex, we have furthermore investigated interactions of the SBS with dsDNA as function of the degree of mechanical underwinding (see below).

In contrast to these strong ssDNA-SBS binding interactions, the dsDNA-SBS experiments show no sign of dsDNA binding to the SBS within the force and time resolution of our instrument (Figures 2C and S2A). This was confirmed in more than 400 interaction experiments with applied forces on the magnetic bead, F_{mag}, in the range F_{mag} = 0.6 – 3 pN and a supercoil density, σ, applied to the dsDNA in the range $\sigma = -0.05$ to +0.02. (Supercoil density is defined as $\sigma = (L - L_0)/L_0$, where L_0 and L are the linking numbers of the relaxed and supercoiled DNA, respectively (Strick et al., 2003). The data confirm that the SBS has a strong preference for ssDNA over dsDNA (Mazin and Kowalczykowski, 1996; Mazin and Kowalczykowski, 1998). Given the force resolution of the dual-molecule technique used here and the maximum forces measured for ssDNA-SBS interactions (>5 pN; see Figure S4), we determine that ssDNA-SBS interaction forces are at least 2 orders of magnitude stronger than dsDNA-SBS interaction forces.

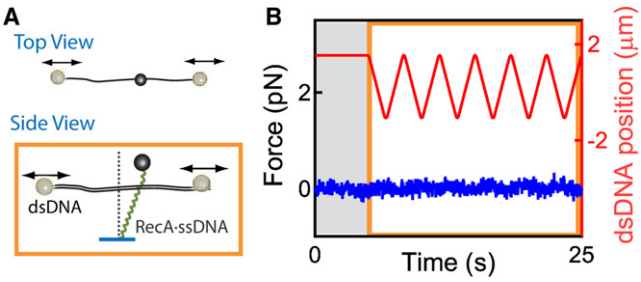

Figure 3. Weak Interactions between dsDNA and RecA·ssDNA

(A) Schematic of side view and top view of the assay for measuring intermolecular friction. Force is measured on the magnetic bead while sliding of a dsDNA across a RecA·ssDNA filament.

(B) Force obtained from the deflection of the magnetic bead (blue trace) and position of the center of the dsDNA tethered in dual-bead optical tweezers before and during the sliding motion (red trace). The force trace indicates frictionless sliding. F_{mag} = 15 pN, F_{opt} = 20 pN. See also Figure S3.

To test whether these weak dsDNA-SBS interactions are a consequence of the presence of dsDNA in the primary site of the filament, interactions were also probed between dsDNA and RecA filaments formed on ssDNA. Figure 3B shows measurements of intermolecular friction that arises during sliding of a dsDNA molecule back and forth across a RecA·ssDNA filament that is held in the magnetic tweezers (configuration III; see schematic in Figure 3A and Movie S2). Before sliding, a contact between both molecules was established by pushing the dsDNA against the RecA filament (Figure S4A). The data in Figure 3B show that the force measured during sliding remains essentially unchanged to the level of the thermal force noise as measured before the start of the sliding movement. These data indicate that dsDNA-SBS interactions are indeed weak, independent of whether ssDNA or dsDNA is present in the primary site. Push-probe measurements with molecules tethered in the same configuration further confirm this observation (see Figure S3C). The previous experiments were carried out in the presence of ATP-γ-s, a poorly hydrolysable analog of ATP. In additional experiments, the effect of RecA-driven ATP-hydrolysis was explored. No evidence of dsDNA-filament interactions was found, independent of whether or not ATP-hydrolysis can occur (Figure S3A). Lastly, our torque-sensitive dual-molecule experiments do not provide evidence for extensive (>1–2 turns) local unwinding of dsDNA at a nonspecific dsDNA-filament contact point (Figure S3B), such as was suggested on the basis of bulk experiments (Rould et al., 1992; Wong et al., 1998).

SBS-ssDNA Interactions Are Too Weak to Allow Stable Trapping of a ssDNA Bubble within dsDNA

To directly compare the free energy of binding of ssDNA to the SBS, ΔG_{SBS}, to the free energy of formation of a B-form DNA duplex, ΔG_B, we studied interactions of underwound dsDNA with the SBS of a RecA filament (configuration I). To this end, a dsDNA molecule tethered in the magnetic tweezers configuration is mechanically coiled while stretched with a stretching force F_{mag} > 1 pN. Figure 4A shows a measurement of the end-to-end distance of a dsDNA as a function of supercoil density at F_{mag} = 3.5 pN. As reported previously (Strick et al., 1996), the curve is highly asymmetric with virtually no coiling dependence of the end-to-end distance for σ < 0. For σ > 0, plectonemes are formed upon coiling, leading to a continuously decreasing end-to-end distance with further coiling. The reason that such plectonemes are not formed for σ < 0, is that mechanical denaturation of the dsDNA is energetically more favorable (Strick et al., 2003). Allemand et al. (1998) have provided evidence for DNA denaturation in undertwisted dsDNA through

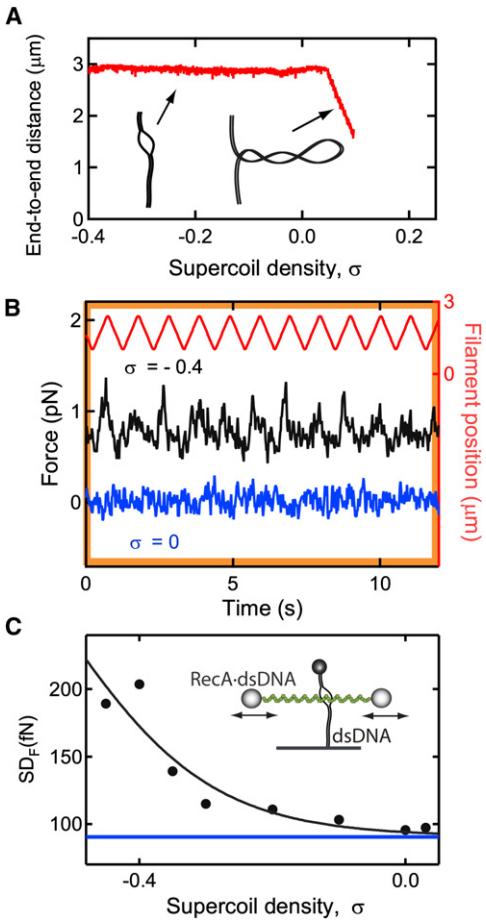

Figure 4. The Affinity of the SBS for ssDNA Is Too Weak to Allow Stable Trapping of ssDNA Bubbles

(A) End-to-end distance versus supercoil density for dsDNA (F_{mag} = 3.5 pN). The curve is highly asymmetric with a weak coiling-number dependence of the end-to-end distance for σ < 0. For σ > 0 and beyond a critical supercoil density, plectonemes are formed upon coiling, leading to a continuously decreasing end-to-end distance with further coiling. For σ < 0, formation of plectonemes is energetically unfavorable, and coiling leads to mechanical denaturation of the dsDNA (Strick et al., 2003).

(B) Measurement of friction during sliding (cf. schematic Figure 3A) of a RecA·dsDNA filament across a mechanically underwound dsDNA (inset in B). Blue trace: frictionless sliding for nonsupercoiled dsDNA (σ = 0). Black trace: friction appears for strongly underwound dsDNA (σ = −0.40, offset for clarity). F_{mag} = 2.5 pN.

(C) Standard deviation (SD) of the measured force, SD_F, (bandwidth 50 Hz) as a function of supercoil density compared to the expected thermal force noise, SD_F, acting on a 1 micron bead: SD_F = 91 fN (bandwidth 50 Hz, blue line). See also Figure S4.

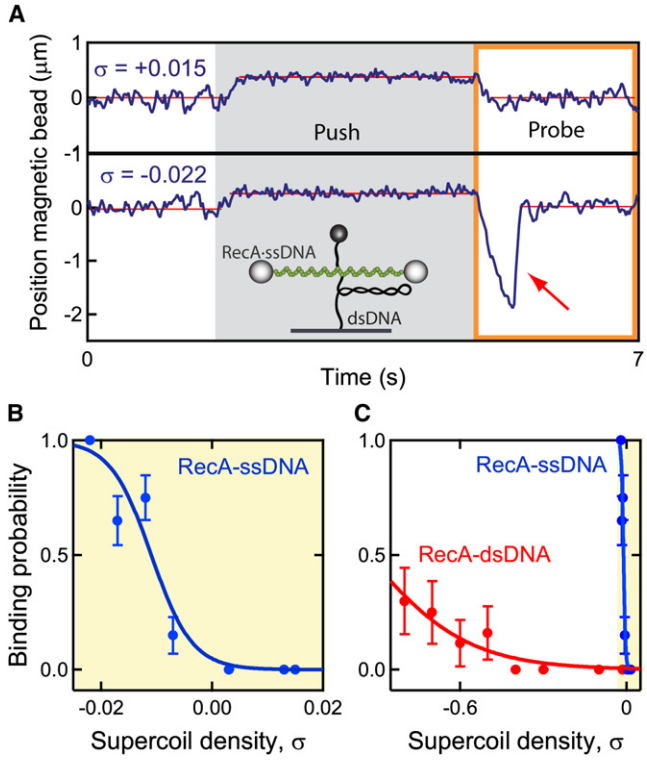

Figure 5. Homologous Pairing Is Strongly Enhanced by Negative Supercoiling

(A) Push-probe experiments (see schematic Figure 2A) reveal binding (red arrow) of a RecA•ssDNA filament to homologous, negatively supercoiled dsDNA (bottom) and absence of binding to positively supercoiled dsDNA (top). F_{mag} = 0.6 pN, F_{opt} = 20 pN.

(B) Binding probability as function of supercoil density. Underwinding of dsDNA strongly promotes the efficiency of pairing. Number of events at each σ, n = 20.

(C) Comparison of binding probability as function of supercoil density for RecA•dsDNA (red, F_{mag} = 2.4 pN, F_{opt} = 20 pN, n = 10) and RecA•ssDNA filaments (blue, data from B). The error bars are calculated as the standard error for a binomial distribution $(P(1 - P)/n)^{1/2}$, where P is the probability of joint-molecule formation. See also Figure S5.

incubation of the DNA with reagents specific for unpaired bases. It was furthermore shown that segments of ssDNA are accessible for binding of single-stranded DNA-binding proteins (De Vlaminck et al., 2010) in mechanically stretched (F_{mag} > 0.5 pN) and underwound dsDNA.

Here, we probe binding of transiently exposed ssDNA segments to the SBS of the filament as function of the degree of uncoiling. Figure 4B shows data of friction during sliding of a RecA•dsDNA filament across torsionally relaxed dsDNA (σ = 0), and across strongly underwound dsDNA (σ = −0.4, F_{mag} = 2.5 pN). At σ = 0, frictionless sliding is observed, i.e., the force measured on the paramagnetic bead equals the thermal noise force. The data for σ = −0.4, however, display stick-slip behavior during sliding, indicative of intermittent intermolecular (un) binding (see also Figures S4D and S4E). The standard deviation of the measured force, SD_F, (Figure 4C) increases beyond the thermal noise value for strong underwinding (σ < −0.2), indicating increasingly stronger intermolecular interactions. Figure 5C (red data points) shows the probability of binding of underwound dsDNA to the SBS of a RecA filament as measured using the push-probe experimental mode. Binding occurs at very high levels of underwinding (σ < −0.4) and the probability of binding increases with increasing levels of underwinding. Intermolecular binding at high levels of underwinding is explained by binding of the SBS to ssDNA that is transiently accessible upon local denaturation of the dsDNA.

An analysis of the statistical distribution of rupture forces, as in Figures 2 and S2, shows that the strength of binding interactions with the SBS are very similar for ssDNA and underwound dsDNA (Figure S4G). This observation further corroborates the interpretation of intermolecular binding during interactions between mechanically underwound dsDNA and a RecA filament as binding of a ssDNA segment that is transiently exposed upon local denaturation of the dsDNA.

The requirement for very high levels of underwinding (>20%) indicates that at more moderate levels of negative supercoiling, binding of ssDNA to the SBS is outcompeted by rebinding to the nearby complementary ssDNA in the denaturation bubble. This shows that ssDNA binding to the SBS is weaker than binding of ssDNA to complementary ssDNA, i.e., $|\Delta G_B| > |\Delta G_{SBS}|$. In other words, the affinity of the SBS for ssDNA is in itself too weak to stably trap ssDNA bubbles in dsDNA.

Homology Recognition Probability Is Strongly Enhanced by DNA Unwinding

To address a potential role for intrinsic DNA-breathing dynamics during base sampling (Voloshin and Camerini-Otero, 2004), we tested whether the probability of homology recognition is enhanced by negative supercoiling of the dsDNA, which is known to strongly promote the frequency of occurrence and lifetime of DNA-breathing bubbles (Jeon et al., 2010; Jeon and Sung, 2008). For these experiments, RecA is assembled on a 20 kb ssDNA that is formed upon mechanical overstretching of a dsDNA molecule (see Figure S5) in the dual-bead optical tweezers (configuration IV), leaving the possibility to twist a homologous dsDNA tethered in the magnetic tweezers. The experimental results (traces in Figure 5A) show a remarkably strong dependence of intermolecular binding on the supercoil density of the dsDNA. At σ = +0.015, no intermolecular binding is observed in a push-probe experiment, whereas at σ = −0.022 a stable joint molecule is formed. Figure 5B shows the probability of joint-molecule formation as a function of σ. It is clear from these data that even slight underwinding of the dsDNA strongly stimulates joint-molecule formation, i.e., binding is not observed at positive supercoiling (σ > 0) whereas 100% probability of binding is observed for σ < −0.015 (n = 20). For a RecA•dsDNA filament, where base-pairing interactions with the DNA in the primary site are excluded and homologous pairing cannot take place, binding events are only observed at much higher levels of negative supercoiling, σ < −0.4 (red data in Figure 5C). The strong dependence of the recognition probability on negative supercoiling points to a model for recognition in which an early step involves the spontaneous breathing dynamics of the donor duplex (Figure 6A) (Wong et al., 1998).

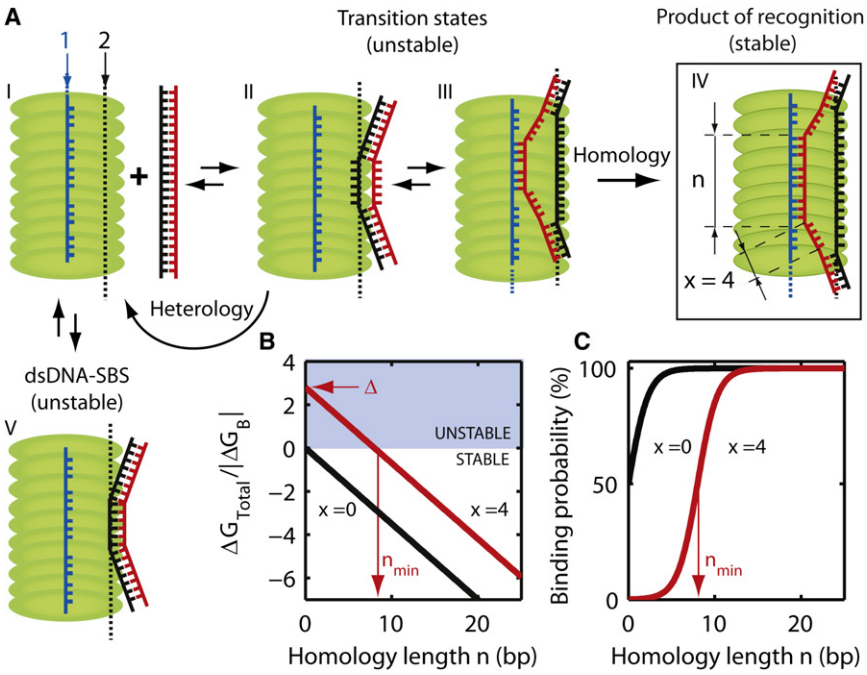

Figure 6. Mechanism of Homology Recognition

(A) Mechanistic model for homology search and recognition. The RecA filament (green) is represented with two binding sites (panel I, indicated 1, 2). A stable joint molecule is formed and homology recognition is achieved when *both* strands of the dsDNA bind to both ssDNA-binding sites in the RecA filament (panel IV). A variety of transition states are accessible along the pathway toward recognition (see examples in panels II–III). Interactions limited to the SBS are unstable and short-lived (panel II). dsDNA-filament interactions are short-lived as well (panel V). For nonhomologous interactions, base paring with the primary site cannot take place, and the transition state (II) will collapse back to the initial state (I).

(B) The reported large distance between the two binding sites (Chen et al., 2008) prevents simultaneous binding to both sites at the edges of the pairing region. This geometrical constraint leads to an energy cost, Δ, that needs to be overcome by the gain in energy in the doubly paired region. This in turn leads to a minimal number of homologous base pairs, n_{min}, required for stable binding to occur. The graph shows the total free energy per bp versus homology length, $\Delta G_{Total} = -(n + 2x)|\Delta G_{SBS}| - n|\Delta G_{HD}| + (n + 2x)|\Delta G_B|$. Introduction of the energy cost Δ shifts the point where $\Delta G_{Total} = 0$ from n = 0 to n = n_{min}. Parameter values used in the model: $|\Delta G_{HD}| = 0.7|\Delta G_B|$, $|\Delta G_{SBS}| = 0.65|\Delta G_B|$; see Supplemental Information.

(C) Binding probability $p(\Delta G_{Total}) = 1/(1+\exp(\Delta G_{Total}/k_bT))$, for ΔG_{Total} in (B). $|\Delta G_B| = 2.5\ k_bT$, with k_b the Boltzmann constant and T the temperature. The finite distance x between the binding sites is seen to have a strong influence. See also Figure S6.

DISCUSSION

Transient Intermediates and Stable Recognition Product

The combined dual-molecule data provide insight into conformations of intermediates of the search and recognition reactions and into the energetics involved in the formation of a stable product of homology recognition. Our measurements showed that ssDNA-SBS interaction forces are at least two orders of magnitude stronger than dsDNA-SBS interaction forces. Since we also find that the affinity of the SBS for ssDNA is weaker than the free energy related to the formation of a B-form DNA duplex, $|\Delta G_B| > |\Delta G_{SBS}|$, we conclude that the affinity of the SBS for dsDNA is too weak to account for local stretching or underwinding of dsDNA during homology sampling. A mechanistic model such as given in Figure 6A is thus preferred, in which the SBS interacts with only a single strand of the incoming dsDNA during homology sampling. Figure 6A shows a reaction pathway from an initial state (panel I), via transient intermediates (panels II–III) to the product of the recognition reaction (panel IV). Short-lived intermediates formed in dsDNA-SBS interactions (panel V, Figure 6A) are unstable transients that do not lead to stable product formation. Since the RecA filament predominantly collides and interacts with heterologous dsDNA during the search process, it is beneficial for the speed of the search that these interactions are indeed weak and short-lived (Radding, 1991; Sagi et al., 2006; Yancey-Wrona and Camerini-Otero, 1995).

On the basis of our dual-molecule data, we can make specific estimates about the energetics of the reaction and the conformation of the stable product of recognition. From the structure of complementary ssDNA bound to the ssDNA in the primary site of the filament, it is known that the incoming complementary ssDNA interacts only weakly with the RecA monomers and that the newly formed heteroduplex is stabilized primarily by Watson-Crick-type base pairing (Chen et al., 2008). The heteroduplex formed within the primary site of the filament adopts a stretched and underwound conformation, resulting in a free energy of binding, $|\Delta G_{HD}|$, which is weaker than the energy of complementary pairing in a nondistorted B-DNA conformation, i.e., $|\Delta G_{HD}| < |\Delta G_B|$. Formation of a stable product thus implies that the loss of binding energy in this less stable conformation, $|\Delta G_B| - |\Delta G_{HD}|$, is compensated by the energy of binding of the other strand of the incoming dsDNA to the SBS, i.e.,

$$|\Delta G_B| - |\Delta G_{HD}| < |\Delta G_{SBS}|. \quad (1)$$

Another inequality is derived from our dual-molecule interaction experiments between underwound dsDNA and the SBS of the filament. Here, the data indicated that ssDNA binding to the SBS is weaker than binding of ssDNA to complementary ssDNA, i.e., $|\Delta G_B| > |\Delta G_{SBS}|$. Since the affinity of the SBS for ssDNA thus is too weak to stably trap ssDNA bubbles in dsDNA, heterologous contacts, where binding is restricted to the SBS, are unstable (panel II, Figure 6A). Combining the above deduced inequalities, $|\Delta G_B| > |\Delta G_{SBS}|$ and $|\Delta G_B| > |\Delta G_{HD}|$, with Equation 1, we thus conclude that:

$$|\Delta G_{SBS}| + |\Delta G_{HD}| > |\Delta G_B| > |\Delta G_{SBS}|, |\Delta G_{HD}|. \quad (2)$$

Stable binding and product formation thus occur exclusively when *both* strands of the incoming dsDNA bind to each of the two independent ssDNA-binding sites of the filament, the sequence-specific ssDNA in the core of the filament and the sequence-nonspecific SBS (Figure S6).

The inequalities in Equation 2 place tight constraints on the possible values of the binding energies of the two ssDNA-binding sites in the filament. By applying the signal-detection formalism developed by Savir and Tlusty (2010) to the present model for homology recognition, we furthermore find that the ability of RecA to discriminate homologous and heterologous sequences is optimal when $|\Delta G_{SBS}|$ and $|\Delta G_{HD}|$ are interdependent, viz. $|\Delta G_{SBS}| = |\Delta G_B| - 0.5|\Delta G_{HD}|$ (see Equation S5 and Figure S6). The condition of optimal recognition thus further restricts the possible free energy values.

Mechanistic Insight into the Minimal Length Required for Homologous Pairing

A remarkable consequence is derived from the above-described model and the large spatial separation (~25 Å) between the primary binding site at the central axis of the filament and the second ssDNA-binding site of the filament (Chen et al., 2008). As a result of this large separation, the strands of the incoming dsDNA can not bind both sites simultaneously over the entire region of pairing. Some bases of one of the strands necessarily remain unpaired at the edges of the pairing region (Figure 6A, panel IV). Since binding to only one of the ssDNA-binding sites does not lead to stable pairing (Equation 2), these two edge regions give rise to an energy cost, Δ, (see Figure 6B) that needs to be compensated for by the gain in binding energy in the central region. This in turn leads to a minimum length of homology, n_{min}, for which stable pairing can occur (Figures 6B and 6C), which is dependent on the distance between both ssDNA-binding sites. Interestingly, under conditions where binding is optimal in the signal-detection formalism, n_{min} simply reads $n_{min} = 2x$, with x the number of unpaired bases (Equations S6 and S7 and Figure S6). For RecA, Hsieh et al. (1992) reported a minimal homology length for stable pairing of 8 bp, corresponding to x = 4 bp, which fits very well with the reported distance between the postulated location of the SBS and the primary site at the filament axis (~25 Å) (Chen et al., 2008). Hsieh et al. exploited the inability of a restriction endonuclease to cleave the duplex within a paired region to probe the homology-length dependence of the probability of homologous pairing. The above-described model directly fits the data by Hsieh et al. remarkably well (see Figure S6H). The analysis furthermore shows that the data by Hsieh et al. is not properly described with a model that does not take into account a finite distance between both binding sites in the filament (black line in Figure 6C).

Such a minimal homology length, n_{min}, explains the ability of RecA to avoid long-term pairing to short (<8 bp) sequences that at random exhibit partial homology and that are abundantly present in the *E. coli* genome (Figure S6). The fidelity of the reaction is thus governed by the physical distance between the SBS and the primary binding site.

dsDNA Is the Active Search Entity

The experiments in Figure 5 directly show that initial homologous pairing does not require a free end of the filament but can occur at any site along a filament. As a result, the search process can be accelerated by a mechanism of parallel search, where homology is sampled at multiple filament-dsDNA contact sites simultaneously (Adzuma, 1998). The model described in Figure 6 is akin to a conformational proofreading scheme (Savir and Tlusty, 2007, 2010) where, interestingly, the dsDNA, and not the RecA filament, is the active, recognizing search entity. A large conformational mismatch exists between the target-bound and unbound states of the dsDNA. The target-bound state is accessed via energetically unfavorable intermediate states, as discussed above. The conformational mismatch improves the selectivity of the recognition reaction.

Dynamics of Helix Opening during Homology Sampling

In our model, formation of a stable recognition product requires opening of the helix over a distance longer than $n_{min} + 2x$ (Figure 6A, panel IV), and the question remains how such long-range helix opening is achieved during homology sampling. Although spontaneous formation of large ssDNA bubbles is energetically unfavorable, thermally activated, long-range opening of the dsDNA helix can take place due to the low energy cost related to the extension of a shorter-range intermediate bubble (Altan-Bonnet et al., 2003; Choi et al., 2004), in particular for AT-rich sequences (Folta-Stogniew et al., 2004; Jeon et al., 2010). ssDNA contacts to one or both of the ssDNA-binding sites in the filament (with free energy of binding values restricted by the inequalities in Equation 2) further lower the extension energy, leading to longer bubble sizes and lifetimes (Figure 6A, example intermediates in panels II–III) (Jeon et al., 2010).

Negative supercoiling promotes helix breathing, explaining the data that showed that homologous pairing is sensitively dependent on negative coiling of the incoming duplex. The strong sensitivity of homologous pairing on supercoiling provides a means for torsional regulation of the reaction, as was similarly proposed for other DNA-metabolic pathways (Choi et al., 2004).

Given the structural and functional similarity of bacterial and eukaryotic recombinases (Kowalczykowski et al., 1994), we anticipate that our results and conclusions also qualitatively apply to the mechanism of homology search and recognition in eukaryotic systems. The dual-molecule technique that was introduced here provides the possibility to interact distinct DNA substrates with great spatial control and allows sensitively probing the effects of torsional stress on intermolecular binding reactions. The technique will be applicable in the study of a wide range of protein-mediated DNA-DNA interactions.

EXPERIMENTAL PROCEDURES

Buffer Conditions

All measurements were carried out at 22°C and were performed in a buffer of 20 mM Tris (pH 6.9), 10 mM NaCl, 13 mM $MgCl_2$, 100 mM DTT. Buffers were filtered (0.22 μm Millipore™ GV filter, PVDF membrane). RecA protein was purchased with New England Biolabs. The experiments were performed in the presence of a poorly hydrolysable ATP-analog (ATP-γ-s) unless otherwise indicated. Experiments with RecA-ssDNA filaments were performed with a low

concentration of RecA (15 nM) in the background to counteract spontaneous RecA disassembly (under ATP and ATP-γ-s conditions).

Force Extraction

Interaction forces in dual-molecule experiments were deduced from the measured in-plane deflection of the magnetic bead along the direction of movement, Δx. Δx is converted into a corresponding rupture force, $F_{x,rupture}$ using:

$$F_{rupture} = \frac{F_{mag}}{h}\Delta x, \quad (3)$$

where h is the height of the contact point measured from the bottom of the flow cell. The height and position of the bead can be measured with high accuracy, δx = 0.5 nm, $\delta z \approx 3$ nm per frame. Given the flexibility of the molecular constructs, there is an uncertainty in the height of the contact point of 100-200 nm (5%–10%). The paramagnetic beads used in this work varies with 5%–10%, force calibrations measurements are subject to a similar level of variability.

SUPPLEMENTAL INFORMATION

Supplemental Information includes six figures, Supplemental Experimental Procedures, Supplemental References, and two movies and can be found with this article online at doi:10.1016/j.molcel.2012.03.029.

ACKNOWLEDGMENTS

We thank Claire Wyman, Roland Kanaar, and Stephen Kowalczykowski for discussions. This work was supported by a DNA-in-action grant from the "Stichting voor Fundamenteel Onderzoek der Materie (FOM)," which is financially supported by the "Nederlandse Organisatie voor Wetenschappelijk Onderzoek (NWO)." Author contributions: I.D.V., M.T.J.v.L., and C.D. designed the experiment. I.D.V., M.T.J.v.L., K.H., J.d.B., and J. K. built the setup; S.H. prepared the DNA constructs; I.D.V. and L.Z. performed the experiments and analysed data; and I.D.V. and C.D. wrote the manuscript. All authors discussed the results and commented on the manuscript.

Received: September 27, 2011
Revised: February 21, 2012
Accepted: March 30, 2012
Published online: May 3, 2012

REFERENCES

Adzuma, K. (1998). No sliding during homology search by RecA protein. J. Biol. Chem. *273*, 31565–31573.

Allemand, J.F., Bensimon, D., Lavery, R., and Croquette, V. (1998). Stretched and overwound DNA forms a Pauling-like structure with exposed bases. Proc. Natl. Acad. Sci. USA *95*, 14152–14157.

Altan-Bonnet, G., Libchaber, A., and Krichevsky, O. (2003). Bubble dynamics in double-stranded DNA. Phys. Rev. Lett. *90*, 138101.

Barzel, A., and Kupiec, M. (2008). Finding a match: how do homologous sequences get together for recombination? Nat. Rev. Genet. *9*, 27–37.

Camerini-Otero, R.D., and Hsieh, P. (1993). Parallel DNA triplexes, homologous recombination, and other homology-dependent DNA interactions. Cell *73*, 217–223.

Chen, Z., Yang, H., and Pavletich, N.P. (2008). Mechanism of homologous recombination from the RecA-ssDNA/dsDNA structures. Nature *453*, 489–4.

Choi, C.H., Kalosakas, G., Rasmussen, K.O., Hiromura, M., Bishop, A.R., and Usheva, A. (2004). DNA dynamically directs its own transcription initiation. Nucleic Acids Res. *32*, 1584–1590.

Danilowicz, C., Feinstein, E., Conover, A., Coljee, V.W., Vlassakis, J., Chan, Y.-L., Bishop, D.K., and Prentiss, M. (2011). RecA homology search is promoted by mechanical stress along the scanned duplex DNA. Nucleic Acids Res. *40*, 1717–1727. Published online October 19, 2011. 10.1093/nar/gkr855.

De Vlaminck, I., Vidic, I., van Loenhout, M.T.J., Kanaar, R., Lebbink, J.H.G., and Dekker, C. (2010). Torsional regulation of hRPA-induced unwinding of double-stranded DNA. Nucleic Acids Res. *38*, 4133–4142.

Dorfman, K.D., Fulconis, R., Dutreix, M., and Viovy, J.-L. (2004). Model of RecA-mediated homologous recognition. Phys. Rev. Lett. *93*, 268102.

Dudko, O.K., Hummer, G., and Szabo, A. (2008). Theory, analysis, and interpretation of single-molecule force spectroscopy experiments. Proc. Natl. Acad. Sci. USA *105*, 15755–15760.

Evans, E. (2001). Probing the relation between force—lifetime—and chemistry in single molecular bonds. Annu. Rev. Biophys. Biomol. Struct. *30*, 105–128.

Folta-Stogniew, E., O'Malley, S., Gupta, R., Anderson, K.S., and Radding, C.M. (2004). Exchange of DNA base pairs that coincides with recognition of homology promoted by E. coli RecA protein. Mol. Cell *15*, 965–975.

Honigberg, S.M., Rao, B.J., and Radding, C.M. (1986). Ability of RecA protein to promote a search for rare sequences in duplex DNA. Proc. Natl. Acad. Sci. USA *83*, 9586–9590.

Hsieh, P., Camerini-Otero, C.S., and Camerini-Otero, R.D. (1992). The synapsis event in the homologous pairing of DNAs: RecA recognizes and pairs less than one helical repeat of DNA. Proc. Natl. Acad. Sci. USA *89*, 6492–6496.

Jeon, J.-H., and Sung, W. (2008). How topological constraints facilitate growth and stability of bubbles in DNA. Biophys. J. *95*, 3600–3605.

Jeon, J.-H., Adamcik, J., Dietler, G., and Metzler, R. (2010). Supercoiling induces denaturation bubbles in circular DNA. Phys. Rev. Lett. *105*, 208101.

Kowalczykowski, S.C., Dixon, D.A., Eggleston, A.K., Lauder, S.D., and Rehrauer, W.M. (1994). Biochemistry of homologous recombination in Escherichia coli. Microbiol. Rev. *58*, 401–465.

Mani, A., Braslavsky, I., Arbel-Goren, R., and Stavans, J. (2010). Caught in the act: the lifetime of synaptic intermediates during the search for homology on DNA. Nucleic Acids Res. *38*, 2036–2043. Published online December 30, 2009. 10.1093/nar/gkp1177.

Mazin, A.V., and Kowalczykowski, S.C. (1996). The specificity of the secondary DNA binding site of RecA protein defines its role in DNA strand exchange. Proc. Natl. Acad. Sci. USA *93*, 10673–10678.

Mazin, A.V., and Kowalczykowski, S.C. (1998). The function of the secondary DNA-binding site of RecA protein during DNA strand exchange. EMBO J. *17*, 1161–1168.

Müller, B., Koller, T., and Stasiak, A. (1990). Characterization of the DNA binding activity of stable RecA-DNA complexes. Interaction between the two DNA binding sites within RecA helical filaments. J. Mol. Biol. *212*, 97–112.

Noom, M.C., van den Broek, B., van Mameren, J., and Wuite, G.J.L. (2007). Visualizing single DNA-bound proteins using DNA as a scanning probe. Nat. Methods *4*, 1031–1036.

Radding, C.M. (1991). Helical interactions in homologous pairing and strand exchange driven by RecA protein. J. Biol. Chem. *266*, 5355–5358.

Rould, E., Muniyappa, K., and Radding, C.M. (1992). Unwinding of heterologous DNA by RecA protein during the search for homologous sequences. J. Mol. Biol. *226*, 127–139.

Sagi, D., Tlusty, T., and Stavans, J. (2006). High fidelity of RecA-catalyzed recombination: a watchdog of genetic diversity. Nucleic Acids Res. *34*, 5021–5031.

Savir, Y., and Tlusty, T. (2007). Conformational proofreading: the impact of conformational changes on the specificity of molecular recognition. PLoS ONE *2*, e468.

Savir, Y., and Tlusty, T. (2010). RecA-mediated homology search as a nearly optimal signal detection system. Mol. Cell *40*, 388–396.

Strick, T.R., Allemand, J.-F., Bensimon, D., Bensimon, A., and Croquette, V. (1996). The elasticity of a single supercoiled DNA molecule. Science *271*, 1835–1837.

Strick, T.R., Dessinges, M.-N., Charvin, G., Dekker, N.H., Allemand, J.F., Bensimon, D., and Croquette, V. (2003). Stretching of macromolecules and proteins. Rep. Prog. Phys. *66*, 1–45.

Voloshin, O.N., and Camerini-Otero, R.D. (2004). Synaptic complex revisited; a homologous recombinase flips and switches bases. Mol. Cell *15*, 846–847.

Wong, B.C., Chiu, S.-K., and Chow, S.A. (1998). The role of negative superhelicity and length of homology in the formation of paranemic joints promoted by RecA protein. J. Biol. Chem. *273*, 12120–12127.

Wuite, G.J.L., Davenport, R.J., Rappaport, A., and Bustamante, C. (2000). An integrated laser trap/flow control video microscope for the study of single biomolecules. Biophys. J. *79*, 1155–1167.

Yancey-Wrona, J.E., and Camerini-Otero, R.D. (1995). The search for DNA homology does not limit stable homologous pairing promoted by RecA protein. Curr. Biol. *5*, 1149–1158.